# Goat Milk Casein Peptides as Potential α-Amylase Inhibitors: A Computational and Experimental Approach

**Gavriel Hagai Paulus Sumlang[1], Rumaisha Lale Handoyo[1], Marlyn Dian Laksitorini[2], Endang Astuti[1], and Tri Joko Raharjo[1*]**

[1]*Department of Chemistry, Faculty of Mathematics and Natural Sciences, Universitas Gadjah Mada, Sekip Utara, Yogyakarta 55281, Indonesia*

[2]*Department of Pharmaceutics, Faculty of Pharmacy, Universitas Gadjah Mada, Sekip Utara, Yogyakarta 55281, Indonesia*

** **Corresponding author:***

*email: trijr_mipa@ugm.ac.id*

*Received: September 27, 2024*
*Accepted: January 4, 2025*

**DOI:** 10.22146/ijc.100223

***Abstract:*** *Goat's milk proteins can undergo hydrolysis during digestion, producing peptides that may inhibit α-amylase and help treat type 2 diabetes with minimal side effects. Identifying the amino acid composition of these peptides is essential for determining their inhibitory potential. Recent* in silico *digestion methods have been developed to generate specific peptides. This study aims to identify α-amylase inhibitory peptides from goat's milk casein hydrolyzate using* in silico *digestion, followed by peptide synthesis and activity assay. Peptides were derived from goat's milk casein hydrolyzed using* in silico *digestion. Molecular docking was employed to predict protein-peptide interactions utilizing the HADDOCK2.4 server, CABS-dock, and PepSite 2 server. Peptides EDVPSER and TNAIPYVR could inhibit α-amylase with $IC_{50}$ values of 14.16 ± 0.65 and 76.58 ± 2.13 μM, respectively.* In vitro *evaluation confirmed that EDVPSER from $\alpha_{S1}$-casein exhibited α-amylase inhibitory potential. This peptide could be developed as a potential therapeutic agent for type 2 diabetes, offering a natural and targeted approach to α-amylase inhibition. Peptide EDVPSER may serve as a basis for further research and development of antidiabetic treatments derived from goat's milk proteins.*

***Keywords:*** *α-amylase;* in silico *digestion; molecular docking; peptide*

## ■ INTRODUCTION

Diabetes mellitus (DM) is known as a serious public health problem with a major impact on human life. Insufficient insulin secretion and insulin resistance are the metabolic disorders that cause DM [1], leading to high blood sugar levels. Type 2 diabetes (T2D) is the most common form of DM. In 2017, it affected approximately 462 million people (6.28% of the global population) and rose from the 18$^{th}$ to the 9$^{th}$ among leading causes of death since 1990 [2].

Several factors, such as unhealthy eating, lack of physical activity, and being overweight are the common risk for developing T2D [3]. There is no effective cure for this metabolic disorder. Treatment of T2D commonly utilizes α-amylase inhibitors as antidiabetics [4]. Several general antidiabetic drugs (e.g., acarbose, metformin, and sulfonylurea) are commercially available to treat T2D, although they show undesired effects, including hypoglycemia, nausea, headache, and gastrointestinal damage [5-6]. Hence, the development of a novel α-amylase inhibitor is urgently required with specific inhibition and minimum side effects.

Several researches have been conducted to inhibit α-amylase performance using peptides from natural products. Recent research shows that the specificity of the peptide's sequence plays an important role in inhibiting α-amylase with a lower $IC_{50}$ value compared to unhydrolyzed protein [7]. Several peptides were investigated and predicted to be active against α-amylase through *in silico* and *in vitro* analyses [8]. The research findings revealed that peptides with amino acids sequence of isoleucine-proline-proline (IPP) showed inhibition of α-amylase with an $IC_{50}$ value of 763.5 ± 18.9 μM. The bioactivity of several peptides was

identified against α-amylase [9]. Peptide YFDEQNEQFR exhibited the highest activity among other peptides, with an $IC_{50}$ value of 37.5 ± 1.1 μM.

Milk holds advantages and impacts on the human body. Goat's milk contains a greater variety of nutrients, such as protein, lipids, water, lactose, vitamins, and minerals [10], compared to cow's milk [11-12]. Casein is the predominant protein in goat's milk, surpassing the amount of whey protein [13]. Its abundance makes goat's milk a promising source of food-derived peptides. This protein contains potential bioactive peptides that could act as α-amylase inhibitors and warrant further development.

*In silico* digestion analysis is a valuable alternative for designing or predicting peptide-based experiments. This analysis also serves as an alternative due to the high costs and time-consuming nature of peptide measurement and characterization. Consequently, the peptide content in natural materials or animal products is often neither thoroughly measured nor analyzed [14]. The identification of bioactive peptides is supported by bioinformatics, which has advanced rapidly, leading to the creation of integrated biological knowledge databases. BIOPEP primarily concentrates on peptides derived from food sources [15].

Detailed structural insights are required to understand the underlying molecular mechanism of protein-peptide interactions. However, experimental characterization has been hindered by the highly dynamic and transient nature of these interactions. As a result, computational methods, particularly protein-peptide docking, have been used as an alternative to predict binding structures [16]. High-Ambiguity Driven Docking (HADDOCK2.4) employs local docking, focusing on modeling and analyzing molecular interactions around specific regions of target proteins [17]. Software like AutoDock Vina, widely used in molecular simulations, does not yield optimal results for protein-peptide interaction predictions due to its energy-based calculations, limitations in handling complex molecules, and restricted receptor flexibility. In contrast, HADDOCK2.4, which utilizes experimental data, accommodates flexible protein-peptide docking. A comprehensive study by [16] demonstrated that HADDOCK2.4 outperformed AutoDock Vina in protein-peptide interaction predictions. The study also emphasizes the importance of using multiple initial peptide conformations to enhance docking performance, suggesting the need for additional tools to support and validate docking results. In this study, protein-peptide interactions were not predicted solely using HADDOCK2.4. Additional servers such as CABS-dock and PepSite 2 were employed for global docking to validate the results [16-19]. The docking was carried out to predict peptide interactions with the catalytic triad of α-amylase, which consists of three coordinated amino acids at the enzyme's active site. These residues, aspartate (Asp197 and Asp300) and glutamate (Glu233), play a key role in carbohydrate breakdown, making them potential inhibitory sites [20-23]. If the peptide interacts with this triad, it could inhibit the enzyme's activity.

## ■ EXPERIMENTAL SECTION

### Materials

The initial protein casein derived from goat's milk was utilized in this study. Several sequences of casein protein, including $\alpha_{S1}$-casein (UniProtKB P18626), $\alpha_{S2}$-casein (UniProtKB P33049), β-casein (UniProtKB P33048), and κ-casein (UniProtKB P02670), were obtained from the UniProt Knowledgebase (www.uniprot.org, accessed in February 2024). The protein used for the molecular docking study was Porcine Pancreatic α-Amylase (PPA). Meanwhile, the three-dimensional (3D) structure was obtained from the Protein Data Bank database (www.rcsb.org, accessed in February 2024) with PDB ID: 1PIF.

The materials and reagents utilized in this experiment included sodium phosphate dibasic dihydrate ($Na_2HPO_4{\cdot}2H_2O$, Merck), sodium phosphate monobasic monohydrate ($NaH_2PO_4{\cdot}H_2O$, Merck), acarbose solids (OGB Dexa), starch substrate solution (Merck), PPA (SRL Chemicals), peptide sample solids (90%, GL Biochem (Shanghai) Ltd.), hydrochloric acid (HCl, 1%, Mallinckrodt), and iodine solution ($I_2$, 0.2%, Merck). The solvents used were distilled water ($H_2O$,

Merck), and dimethyl sulfoxide solution (DMSO, Merck). All solvents were of analytical grade.

## Instrumentation

The presence of amylum was analyzed using a UV-vis spectrophotometer (Thermo Scientific Evolution).

## Procedure

### In silico *digestion of goat's milk casein*

The amino acid sequences of goat's milk casein were obtained from the UniProtKB. There are four types of casein in goat's milk: $\alpha_{S1}$-casein, $\alpha_{S2}$-casein, β-casein, and κ-casein. Each type of casein was then subjected to *in silico* digestion using the Expasy PeptideMass (web.expasy.org/peptide_mass, accessed in March 2024) with trypsin as the enzyme. The peptides containing between 4 to 10 amino acids were selected. The previous activity of these peptides was then identified using the BIOPEP-UWM (biochemia.uwm.edu.pl/biopep/sensory_data.php, accessed in March 2024). Subsequently, the peptides were scored using the PeptideRanker (distilldeep.ucd.ie/PeptideRanker, accessed in March 2024) and the PepSite 2 (pepsite2.russelllab.org, accessed in March 2024). Those meeting the criteria from each server were predicted to be bioactive peptides.

### *Preparation of protein and peptides*

The 3D structure of α-amylase (PDB ID: 1PIF, 2.30 Å) was prepared using UCSF Chimera. The protein was cleaned from water molecules and native ligands. The peptides obtained through *in silico* methods were then utilized to design their three-dimensional structures. These *de novo* peptide structures were generated using the PEP-FOLD4 (bioserv.rpbs.univ-paris-diderot.fr/services/PEP-FOLD4, accessed in March 2024). The best peptide model was selected for docking analysis. The lowest Optimized Potential for Efficient Structure Prediction (sOPEP) score indicates the most favorable conformation of the peptide.

### *Protein-peptide molecular docking*

Docking was performed using HADDOCK2.4 (rascar.science.uu.nl/haddock2.4, accessed in March 2024) [24-25] and CABS-dock (biocomp.chem.uw.edu.pl/CABSdock, accessed in March 2024) [26]. Docking on the HADDOCK server required the amino acid sequences of the receptor protein's active site and the peptides as input data. Meanwhile, docking on the CABS-dock server required the 3D structure of protein and peptide sequence as input data. The best cluster was selected from both servers. Then, the binding affinity energy predictions from the docking results were performed using PRODIGY (rascar.science.uu.nl/prodigy, accessed in March 2024).

### *Secondary structure analysis*

The Structure-based Empirical Spectrum Calculation Algorithm (SESCA) software was employed to analyse the secondary structure of the peptides. This analysis required protein and peptide sequences as input. SESCA was executed using Python 3.11 through a single script, SESCA_main. The SESCA data obtained were then processed to generate secondary structure prediction.

### *Synthesis of peptides*

The peptide with the best docking results was selected for synthesis, which was performed by GL. Biochem (Shanghai) Ltd. using solid-state synthesis. Each peptide was synthesized in a quantity of 20 mg with a purity of over 90%. The physicochemical properties of the obtained peptides were examined using the Peptide Property Calculator (pepcalc.com, accessed in March 2024) and Expasy ProtParam (web.expasy.org/protparam, accessed in March 2024).

### In vitro *antidiabetic activity assay of α-amylase inhibitors*

The synthesized peptides were dissolved in 0.1 M phosphate buffer ($Na_2HPO_4{\cdot}2H_2O$ and $NaH_2PO_4{\cdot}H_2O$ at pH 6.9 and 1.0 mL of DMSO to achieve a final concentration of 500 ppm). The peptide sample solutions were prepared by diluting the 500 ppm to various concentrations: 400, 300, 200, 100, 50, and 25 ppm. The activity assay was conducted on different systems with identical treatments ($S_0$, $S_1$, blank, and control).

The antidiabetic activity assay was carried out by mixing 100 µL of starch substrate with 20 µL of the peptide sample solution. Furthermore, 20 µL of α-amylase solution was added to the mixture. The solution

was then incubated at 37 °C for 15 min. To terminate the reaction, 20 µL of 1% HCl was added, followed by 2 µL of 0.2% $I_2$ solution to each sample. The absorbance of the $S_0$ mixed solution was measured using a UV-vis spectrophotometer at a maximum wavelength of 540 nm with 3 replicates. The comparative solution used was 500 ppm acarbose. The percentage inhibition was calculated using the following Eq. (1);

$$\alpha-\text{amylase inhibition (\%)} = \frac{\text{Abs(blank}-\text{control)}-\text{Abs}(S_0-S_1)}{\text{Abs(blank}-\text{control)}}\times 100\% \quad (1)$$

where $S_1$ is the absorbance of the system containing the substrate, enzyme, and sample; $S_0$ represents $S_1$ without the enzyme, control corresponds to $S_1$ without the sample; blank refers to the absorbance of the system containing only the substrate. The percentage inhibition of peptides at each concentration and each replicate was converted to $IC_{50}$ value, at which inhibition reached 50%. The value obtained was expressed in µM to account for the peptide's molecular weight.

## ■ RESULTS AND DISCUSSION

### *In Silico* Digestion of Goat's Milk Casein

Casein was chosen as the source of bioactive peptides because it is the most abundant protein in goat's milk [13]. The discovery of bioactive peptides was predicted based on the number of peptides generated from *in silico* digestion and the specific molecular weight of peptides [14]. The main casein protein in goat's milk comprises $\alpha_{S1}$-casein, $\alpha_{S2}$-casein, β-casein, and κ-casein. Table 1 provides information related to protein mass and the number of amino acids in each protein. According to Table 1, among the proteins, $\alpha_{S2}$-casein and κ-casein had the highest and lowest masses, respectively. Those proteins were then hydrolyzed by *in silico* digestion. As reported in Table 2, a total of 57 peptide fragments were obtained from $\alpha_{S1}$-casein, $\alpha_{S2}$-casein, β-casein, and κ-casein. The results of the *in silico* digestion showed that each protein of $\alpha_{S1}$-casein, $\alpha_{S2}$-casein, β-casein, and κ-casein generated 16, 20, 12, and 9 peptide fragments, respectively. It indicates that $\alpha_{S2}$-casein and κ-casein had the highest and lowest number of peptide fragments per molecule, respectively.

A total of 24 peptides were chosen for molecular docking. Peptides with 4–10 amino acids were selected because smaller peptides often have higher bioactivity, e.g. neuropeptide [27], antioxidative [28], and even DPP IV inhibitor [29]. Furthermore, peptides with fewer than 4 amino acids could not be used due to tool limitations. BIOPEP-UWM identified 8 peptides with known biological activity, while 16 had unknown activity. Peptides from $\alpha_{S2}$-casein showed no activity, and none of the peptides inhibited α-amylase. The active peptides are listed in Table 3.

**Table 1.** Protein mass and number of amino acids in each casein protein

| Casein protein | Mass (Da) | The number of amino acids |
|---|---|---|
| $\alpha_{S1}$-casein | 24.290 | 214 |
| $\alpha_{S2}$-casein | 26.389 | 223 |
| β-casein | 24.865 | 222 |
| κ-casein | 21.441 | 192 |

**Table 2.** Number of peptide fragments obtained from in silico digestion of casein protein of goat's milk

| Peptide mass (Da) | Amino acids sequence | Number of amino acids |
|---|---|---|
| $\alpha_{S1}$-casein | | |
| 4,658.17 | QFYQLDAYPSGAWYYLPLGTQYTDAPSFDIPNPIGSENSGK | 42 |
| 2,328.19 | QPMIAVNQELAYFYPQLFR | 19 |
| 1,806.83 | AGSSSSSEEIVPNSAEQK | 18 |
| 1,725.71 | DIGSESTEDQAMEDAK | 16 |
| 1,694.08 | LLILTCLVAVALARPK | 16 |
| 1,437.77 | GLSPEVPNENLLR | 13 |
| 1,307.71 | FVVAPFPEVFR | 11 |
| 1,299.73 | YNVPQLEIVPK | 11 |
| 1,267.70 | YLGYLEQLLR | 10 |

| Peptide mass (Da) | Amino acids sequence | Number of amino acids |
|---|---|---|
| 1,159.54 | SAEEQLHSMK | 10 |
| 946.48 | ENINELSK | 8 |
| 880.43 | EGNPAHQK | 8 |
| 831.38 | EDVPSER | 7 |
| 773.42 | HPINHR | 6 |
| 748.37 | TTMPLW | 6 |
| 551.32 | YIQK | 4 |
| $\alpha_{S2}$-casein | | |
| 2,693.38 | FPQYLQYPYQGPIVLNPWDQVK | 22 |
| 2,280.08 | MEHVSSSEEPINIFQEIYK | 19 |
| 1,591.73 | SSSEESAEVAPEEIK | 15 |
| 1,556.89 | FFIFTCLLAVALAK | 14 |
| 1,400.66 | TIDMESTEVFTK | 12 |
| 1,367.69 | ALNEINQFYQK | 11 |
| 1,251.57 | EQLSTSEENSK | 11 |
| 1,239.57 | LCTTSCEEVVR | 11 |
| 1,224.55 | NANEEEYSIR | 10 |
| 1,173.60 | NAGPFTPTVNR | 11 |
| 1,086.58 | AMKPWTQPK | 9 |
| 1,052.56 | FAWPQYLK | 8 |
| 933.51 | TNAIPYVR | 8 |
| 929.47 | ISQYYQK | 7 |
| 855.43 | TVDQHQK | 7 |
| 838.43 | NMAIHPR | 7 |
| 748.37 | LTEEEK | 6 |
| 690.37 | ITVDDK | 6 |
| 634.39 | LNFLK | 5 |
| 575.29 | HYQK | 4 |
| β-casein | | |
| 5,330.90 | IHPFAQAQSLVYPFTGPIPNSLPQNILPLTQTPVVVPPFLQP EIMGVPK | 49 |
| 4,155.23 | LHLPLPLVQSWMHQPPQPLSPTVMFPPQSVLSLSQPK | 37 |
| 2,987.43 | EQEELNVVGETVESLSSSEESITHINK | 27 |
| 2,186.17 | DMPIQAFLLYQEPVLGPVR | 19 |
| 2,183.07 | YPVEPFTESQSLTLTDVEK | 19 |
| 1,981.86 | FQSEEQQQTEDELQDK | 16 |
| 1,438.92 | VLILACLVALAIAR | 14 |
| 780.50 | VLPVPQK | 7 |
| 748.37 | EMPFPK | 6 |
| 742.45 | GPFPILV | 7 |
| 704.36 | ETMVPK | 6 |
| 570.34 | AVPQR | 5 |
| κ-casein | | |
| 5,569.67 | TEVPAINTIASAEPTVHSTPTTEAIVNTVDNPEASSESIASASETNTAQVTSTEV | 55 |
| 4,066.10 | YPSYGLNYYQQRPVALINNQFLPYPYYAKPVAVR | 34 |
| 3,479.79 | SFFLVVTILALTLPFLGAQEQNQEQPICCEK | 31 |
| 1,978.08 | SPAQTLQWQVLPNTVPAK | 18 |

| Peptide mass (Da) | Amino acids sequence | Number of amino acids |
|---|---|---|
| 1,608.85 | HPHPHLSFMAIPPK | 14 |
| 1,251.71 | YIPIQYVLSR | 10 |
| 1,219.57 | SCQDQPTTLAR | 11 |
| 671.30 | FFDDK | 5 |
| 505.22 | DQDK | 4 |

**Table 3.** Peptides generated by *in silico* digestion and their activity in the human body

| Amino acids sequence | Activity | Ref. |
|---|---|---|
| $\alpha_{S1}$-casein | | |
| YLGYLEQLLR | Anxiolytic-like | [27] |
| EDVPSER | Osteoanabolic | [30] |
| | Antioxidative | [28] |
| HPINHR | DPP IV inhibitor | [29] |
| TTMPLW | Antibacterial | [31] |
| | Antifungal | [31] |
| β-casein | | |
| VLPVPQK | Antibacterial | [32] |
| | Antioxidative | [28] |
| | Osteoanabolic | [30] |
| | Anti-apoptotic | [33] |
| | DPP IV inhibitor | [29] |
| | Stimulating | [34] |
| EMPFPK | Stimulating | [35] |
| | Antibacterial | [32] |
| GPFPILV | DPP IV inhibitor | [29] |
| κ-casein | | |
| YIPIQYVLSR | Opioid antagonist | [36] |

Bioactivity predictions for 24 peptides were carried out using PeptideRanker and PepSite 2. Those with low significance values were likely to bind to the α-amylase active site, blocking its activity. Table 4 exhibits the results of the screening. Six peptides with PeptideRanker scored above 0.5 were predicted to have bioactivity (ranging from 0.56 to 0.90). In addition, PepSite 2 analysis showed low p-values for these peptides, indicating strong binding potential. These peptides were predicted to be bioactive based on *in silico* screening.

## Protein-Peptide Molecular Interactions

Docking simulations were performed on 24 peptides from *in silico* digestion against α-amylase to evaluate their interactions. The α-amylase was used as the receptor due to its 90% similarity to human pancreatic α-amylase [22]. This enzyme has 496 amino acids divided into three domains: A (residues 1-99, 169-404, with $Cl^-$), B (residues 100-168, with $Ca^{2+}$), and C (residues 405-496). It also includes pyroglutamic acid (PCA) as a small molecule residue. Fig. 1 shows the 3D structure of α-amylase visualized using DSV Biovia 2020.

Molecular docking of 24 peptides produced clustering and HADDOCK scores. Table 5 demonstrates the best HADDOCK scores for each peptide. Docking results were validated through root mean square deviation (RMSD) and Z-score calculations, which aided in identifying the most accurate clusters [37]. The best clusters confirmed consistent peptide docking with α-amylase under natural conditions. HADDOCK scores alone cannot determine the best peptide inhibitor for α-amylase. They only identify the best conformations based on RMSD values. Low RMSD indicates stable

**Table 4.** Peptide bioactivity predicted by PeptideRanker and PepSite 2

| Amino acids sequence | PeptideRanker score | PepSite 2 | |
|---|---|---|---|
| | | *p*-value | Binding site |
| FAWPQYLK | 0.91 | 0.0019 | 6 of 8 amino acids |
| GPFPILV | 0.87 | 0.0712 | 4 of 7 amino acids |
| EMPFPK | 0.77 | 0.0031 | 5 of 6 amino acids |
| FFDDK | 0.75 | 0.0372 | 4 of 5 amino acids |
| TTMPLW | 0.74 | 0.0119 | 5 of 6 amino acids |
| LNFLK | 0.56 | 0.0147 | 4 of 5 amino acids |

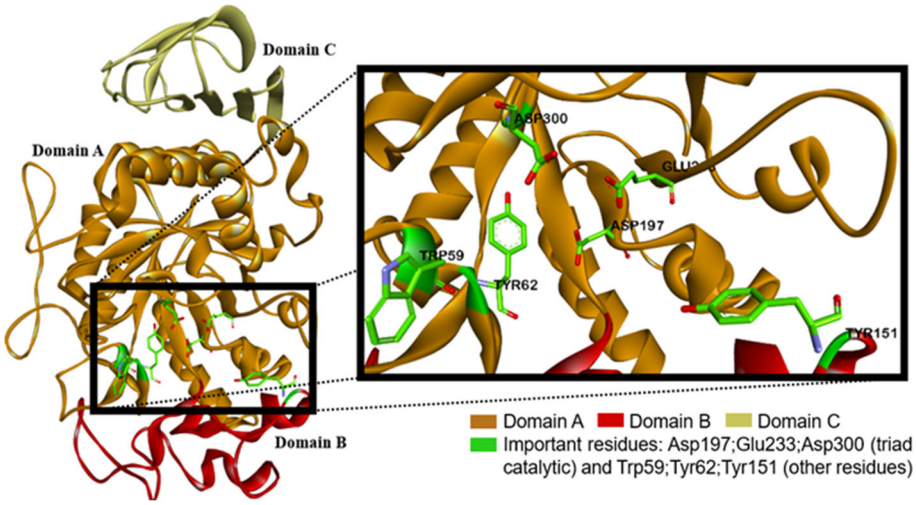


**Fig 1.** Visualization of the 3D structure of α-amylase and important amino acids in starch hydrolysis

**Table 5.** Clustering of peptides based on HADDOCK score

| Amino acids sequence | Cluster | HADDOCK score | RMSD (Å) | Z-score |
|---|---|---|---|---|
| $\alpha s_1$-casein | | | | |
| YLGYLEQLLR | 1 | -81.4 ± 1.2 | 0.9 ± 0.0 | -1.7 |
| SAEEQLHSMK | 7 | -81.1 ± 4.5 | 0.1 ± 0.1 | -1.7 |
| ENINELSK | 2 | -63.1 ± 1.7 | 0.6 ± 0.1 | -1.5 |
| EGNPAHQK | 1 | -67.2 ± 2.3 | 0.2 ± 0.1 | -1.3 |
| EDVPSER | 3 | -62.7 ± 6.1 | 0.2 ± 0.1 | -1.3 |
| HPINHR | 2 | -74.2 ± 2.6 | 0.9 ± 0.1 | -1.6 |
| TTMPLW | 1 | -70.2 ± 4.4 | 0.2 ± 0.1 | -1.9 |
| $\alpha s_2$-casein | | | | |
| NANEEEYSIR | 3 | -72.4 ± 4.7 | 0.4 ± 0.2 | -1.7 |
| AMKPWTQPK | 4 | -80.5 ± 3.7 | 1.4 ± 0.0 | -1.2 |
| FAWPQYLK | 1 | -99.9 ± 1.9 | 0.2 ± 0.1 | -1.5 |
| TNAIPYVR | 2 | -60.4 ± 0.5 | 1.2 ± 0.1 | -1.8 |
| ISQYYQK | 3 | -89.1 ± 6.9 | 0.4 ± 0.2 | -1.8 |
| TVDQHQK | 6 | -69.1 ± 4.0 | 0.1 ± 0.1 | -1.8 |
| NMAIHPR | 1 | -72.3 ± 2.8 | 0.3 ± 0.2 | -2.3 |
| LTEEEK | 2 | -62.2 ± 9.1 | 0.4 ± 0.2 | -1.8 |
| ITVDDK | 1 | -59.1 ± 2.1 | 0.9 ± 0.1 | -1.8 |
| LNFLK | 1 | -68.9 ± 0.4 | 0.5 ± 0.2 | -1.5 |
| β-casein | | | | |
| VLPVPQK | 2 | -74.5 ± 0.9 | 1.1 ± 0.0 | -1.7 |
| EMPFPK | 5 | -78.4 ± 7.5 | 0.3 ± 0.2 | -2.1 |
| GPFPILV | 2 | -63.0 ± 5.4 | 0.2 ± 0.1 | -2.1 |
| ETMVPK | 1 | -50.4 ± 6.2 | 0.3 ± 0.2 | -1.6 |
| AVPQR | 9 | -50.7 ± 4.3 | 0.2 ± 0.1 | -1.8 |
| κ-casein | | | | |
| YIPIQYVLSR | 1 | -79.8 ± 4.3 | 0.5 ± 0.1 | -1.5 |
| FFDDK | 6 | -81.3 ± 5.4 | 0.2 ± 0.1 | -1.3 |

conformations close to the reference model (optimization structure). Further analysis of binding affinity and protein-peptide interactions is needed to predict inhibitory activity.

Table 6 presents the predicted binding affinity energies and hydrogen bond interactions between peptides and α-amylase. Out of 24 docked peptides, 19 formed hydrogen bond interactions with the catalytic triad. The peptide TVDQHQK had the lowest binding affinity (ΔG = −10.9 kcal/mol) but formed only 4 hydrogen bonds, none of which involved the catalytic triad. In contrast, peptides TNAIPYVR (ΔG = −9.3 kcal/mol) and EDVPSER (ΔG = −9.2 kcal/mol) formed 7 hydrogen bonds, three of which interacted with the catalytic triad. These peptides are predicted to bind stably and potentially inhibit α-amylase.

Peptides TNAIPYVR and EDVPSER were preferred over TVDQHQK, despite having higher binding affinity energies. Their selection was based on hydrogen bond interactions, as a greater number of interactions enhances the stability of the protein-peptide complex than a single and stronger hydrogen bond interaction [38]. Additionally, the ability of peptides to interact with the enzyme's active site is crucial for inhibition [6]. Further analysis of the protein-peptide interactions was conducted using additional supporting servers.

Fig. 2 shows the molecular docking results for the peptide EDVPSER with α-amylase, revealing hydrogen bond interactions with 7 amino acid residues. The C-terminal glutamic acid (E) interacted with Trp357 via its carbonyl oxygen. The hydroxyl hydrogen of serine (S) formed a bond with His305. Another glutamic acid (E)

**Table 6.** Docking results of all peptides with α-amylase predicted by HADDOCK2.4

| Amino acids sequence | ΔG (kcal/mol) | Hydrogen bond | Total of hydrogen bond |
|---|---|---|---|
| $\alpha_{s1}$-casein | | α-amylase | |
| YLGYLEQLLR | −9.3 | Trp59, Lys200, Gly238, Glu240, Asp300*, Asp356 | 6 |
| ENINELSK | −10.6 | Gln63, His101, Tyr151, Val163, Asp197*, His305 | 6 |
| EGNPAHQK | −8.9 | Lys200, Ile235, Asp300*, Glu352 | 4 |
| EDVPSER | −9.2 | Tyr151, Val163, Asp197*, Glu233*, Asp300*, His305, Trp357 | 7 |
| HPINHR | −10.5 | Tryr151, Asp197*, Glu240, Asp300*, Gly308 | 5 |
| TTMPLW | −8.5 | Val50, Trp58, Gln63, Asp300*, Asp356 | 5 |
| $\alpha_{s2}$-casein | | α-amylase | |
| NANEEEYSIR | −10.5 | Val163, Gly238, Glu240, Asp300* | 4 |
| FAWPQYLK | −8.4 | His305, Asp300* | 2 |
| TNAIPYVR | −9.3 | Glu149, Asp197*, Glu233*, Asp300*, Glu352, Asp353, Asp356 | 7 |
| ISQYYQK | −10.2 | Tyr151, Glu240, Asp300*, His305, Gly306, Asp356 | 6 |
| TVDQHQK | −10.9 | Ile148, Glu240, Glu240, Ala307 | 4 |
| NMAIHPR | −9.2 | Ile148, Val163, Asp197*, Lys200, Glu233* | 5 |
| LTEEEK | −9.7 | Tyr151, Val163, Asp197*, His201, Glu233*, Ala307 | 6 |
| LNFLK | −8.2 | Glu233* | 1 |
| β-casein | | α-amylase | |
| VLPVPQK | −8.9 | Asp300*, Gly306, Asp356 | 3 |
| EMPFPK | −8.7 | Asp300*, His305 | 2 |
| GPFPILV | −7.6 | Gln63, Asp300* | 2 |
| AVPQR | −9.3 | Tyr151, His299, Asp300*, His305 | 4 |
| κ-casein | | α-amylase | |
| YIPIQYVLSR | −9.8 | Trp58, Glu240, Asp300* | 3 |

*Catalytic triad of α-amylase

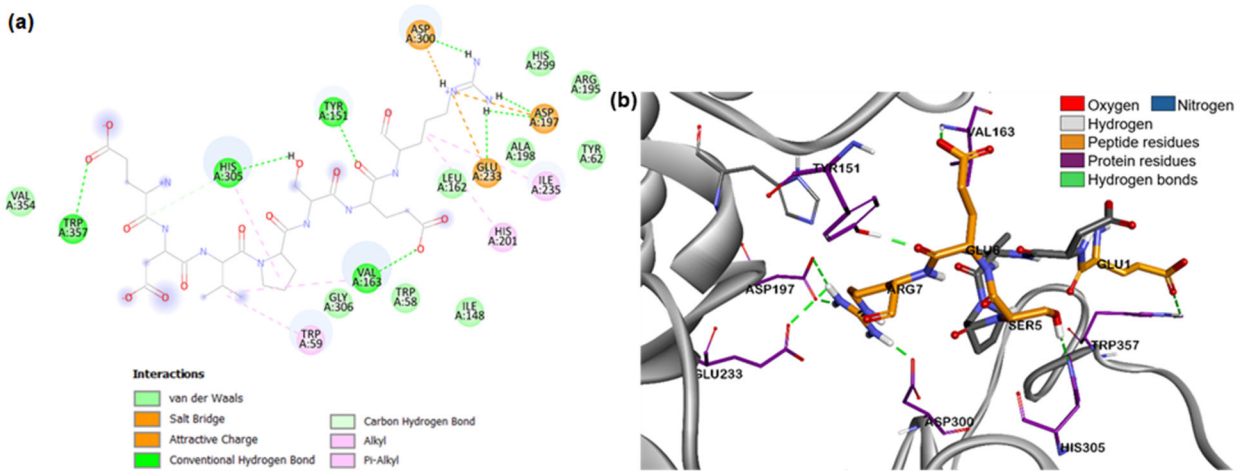


**Fig 2.** Interaction analysis of peptide EDVPSER with α-amylase from HADDOCK2.4 generated by DSV Biovia 2020: (a) 2D interaction map binding to the active site of α-amylase (Asp197, Glu233, and Asp300) and (b) 3D binding model of peptide EDVPSER in complex with α-amylase

interacted with Tyr151 via its carbonyl oxygen, and the carboxyl oxygen bonded with Val163. The *N*-terminal arginine (R) formed three hydrogen bonds: two with Asp197 and one with Glu233 through its guanidine amine groups, while another amine group bonded with Asp300. These interactions included the catalytic triad.

The prediction results of EDVPSER using PepSite 2 are presented in Table 7. Based on these results, the peptide EDVPSER had the lowest p-value of 0.01245, with 6 interacting amino acid residues including Asp2, Val3, Pro4, Ser5, Glu6, and Arg7. This prediction differed from the results produced by the HADDOCK2.4 server.

The prediction results of EDVPSER using CABS-dock are presented in Table 8. A total of 42 interactions were formed between the peptide EDVPSER and α-amylase. Among these interactions, nine protein-peptide interactions were observed with the catalytic triad of α-amylase. The amino acid residues of the peptide that interacted with the catalytic triad of α-amylase were Glu1, Pro4, Ser5, and Glu6. These interaction results varied from the predictions generated by the HADDOCK2.4 and PepSite 2 servers.

Fig. 3 displays the molecular docking results for the peptide TNAIPYVR with α-amylase, revealing hydrogen bond interactions with 7 amino acid residues. The C-terminal threonine (T) formed bonds with Glu233 (hydroxyl hydrogen) and Asp197 (amine hydrogen). Alanine (A) formed a bond with Asp300 (amine hydrogen), while tyrosine (Y) bonded with Glu149 (hydroxyl hydrogen). Meanwhile, the *N*-terminal arginine (R) formed three hydrogen bonds via its guanidine amine groups: two with Asp353, Glu352, and Asp356, and one with Asp356 and Glu352. In addition, interactions with the α-amylase catalytic triad were also observed.

**Table 7.** Amino acid active sites of EDVPSER interacting with α-amylase predicted by PepSite 2

| *p-value* | N | 1 | 2 | 3 | 4 | 5 | 6 | 7 |
|---|---|---|---|---|---|---|---|---|
| 0.01245 | 6 | - | Asp | Val | Pro | Ser | Glu | Arg |

**Table 8.** Amino acid interactions of EDVPSER interacting with α-amylase predicted by CABS-dock

| Receptor residue | Peptide residue | Receptor residue | Peptide residue | Receptor residue | Peptide residue |
|---|---|---|---|---|---|
| Ala307 | Asp2 | Ala307 | Ser5 | Arg337 | Glu6 |
| Asn301 | Ser5 | His305 | Asp2 | Gly306 | Asp2 |
| Asp300* | Pro4 | Asp300* | Ser5 | Asp300* | Glu6 |
| His299 | Glu6 | His299 | Arg7 | Asp300* | Glu1 |

| Receptor residue | Peptide residue | Receptor residue | Peptide residue | Receptor residue | Peptide residue |
|---|---|---|---|---|---|
| Thr254 | Glu6 | Asn298 | Ser5 | Asn298 | Glu6 |
| Ile235 | Val3 | Ile235 | Pro4 | Ile235 | Ser5 |
| Glu233* | Ser5 | Glu233* | Glu6 | Ile235 | Asp2 |
| His201 | Val3 | His201 | Pro4 | Glu233* | Pro4 |
| Asp197* | Pro4 | Ala198 | Pro4 | Ser199 | Pro4 |
| Val163 | Glu1 | Arg195 | Glu6 | Arg195 | Arg7 |
| Asp96 | Arg7 | Ile148 | Val3 | Tyr151 | Val3 |
| Pro44 | Arg7 | Trp59 | Glu1 | Tyr62 | Pro4 |
| Gln41 | Arg7 | Val42 | Arg7 | Ser43 | Arg7 |
| His15 | Arg7 | Leu16 | Arg7 | Phe17 | Arg7 |

*Catalytic triad of α-amylase

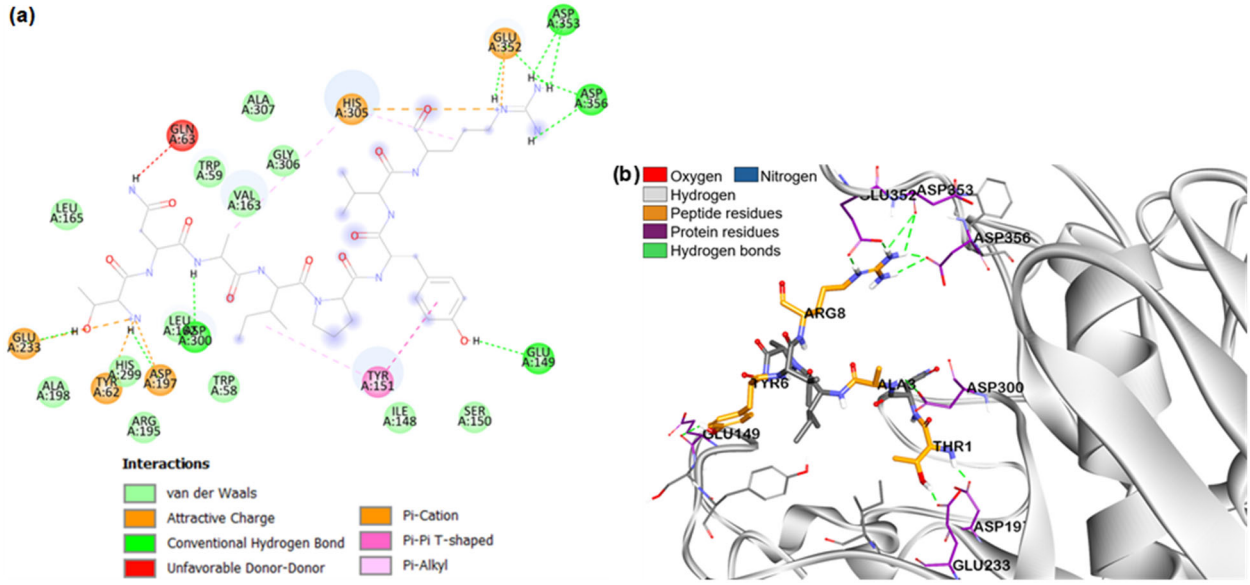


**Fig 3.** Interaction analysis of peptide TNAIPYVR with α-amylase from HADDOCK2.4 generated by DSV Biovia 2020: (a) 2D interaction map binding to the active site of α-amylase (Asp197, Glu233, and Asp300) and (b) 3D binding model of peptide TNAIPYVR in complex with α-amylase

**Table 9.** Amino acid active sites of TNAIPYVR interacting with α-amylase predicted by PepSite 2

| *p-value* | N | 1 | 2 | 3 | 4 | 5 | 6 | 7 | 8 |
|---|---|---|---|---|---|---|---|---|---|
| 0.03736 | 5 | - | Asn | Ala | - | Pro | Tyr | - | Arg |

The prediction of TNAIPYVR results obtained using PepSite 2 is presented in Table 9. It can be seen that the peptide TNAIPYVR had the lowest p-value of 0.03736, with interactions involving five amino acid residues: Asn2, Ala3, Pro5, Tyr6, and Arg8. This prediction differed from the results acquired through the HADDOCK2.4 server.

The prediction results of TNAIPYVR obtained using CABS-dock are presented in Table 10. A total of 36 interactions were formed between the peptide TNAIPYVR and α-amylase. The results indicate that all amino acid residues of the peptide TNAIPYVR interact with residues from the receptor. Among these, 10 protein-peptide interactions were formed with the catalytic triad of α-amylase. The amino acid residues of the peptide interacting with the catalytic triad of α-amylase were Thr1, Asn2, Ala3, Ile4, and Pro5. These interaction results differed from the predictions generated

by the HADDOCK2.4 and PepSite 2 servers.

The molecular docking results obtained using the HADDOCK2.4, CABS-dock, and PepSite 2 servers showed differing interaction patterns. These variations in results are due to the different protocols and algorithms employed by each server. However, based on these docking results, it can be concluded that the molecular docking of protein-peptides revealed hydrogen bond interactions with the catalytic triad amino acids of α-amylase. Computationally, the inhibition is indicated by the interactions with these catalytic triad amino acids. Nevertheless, experimental validation in the laboratory is required to confirm their activity.

## Secondary Structure of Peptides Analysis

Predicting the secondary structure of peptides is vital for understanding their three-dimensional conformation and protein-peptide interactions. Circular Dichroism (CD) spectroscopy, a widely used method, estimates secondary structures such as α-helix, β-sheet, and random coil by detecting wavelength differences in the absorption of circularly polarized light by optically active molecules [39]. Using SESCA, CD spectroscopy provides insights into peptide and protein backbone structures at 270–175 nm.

Fig. 4 shows the predicted Circular Dichroism spectra for the peptides EDVPSER and TNAIPYVR, with

**Table 10.** The predicted amino acid interactions between TNAIPYVR and α-amylase using CABS-dock

| Receptor residue | Peptide residue | Receptor residue | Peptide residue | Receptor residue | Peptide residue |
|---|---|---|---|---|---|
| Ala307 | Ile4 | His305 | Arg8 | Gly306 | Pro5 |
| Asn301 | Ile4 | Asp300* | Ile4 | Asp300* | Pro5 |
| Asp300* | Ala3 | Asp300* | Thr1 | Asp300* | Asn2 |
| His299 | Thr1 | Asn298 | Thr1 | Asn298 | Ile4 |
| Phe256 | Ile4 | Ile235 | Arg8 | Glu240 | Arg8 |
| Ile235 | Val7 | Glu233* | Pro5 | Ile235 | Ile4 |
| Glu233* | Ile4 | His201 | Val7 | Glu233* | Ala3 |
| His201 | Tyr6 | Ala198 | Tyr6 | Lys200 | Val7 |
| Asp197* | Ala3 | Arg195 | Thr1 | Asp197* | Thr1 |
| Leu165 | Tyr6 | Leu162 | Tyr6 | Leu162 | Val7 |
| Tyr151 | Arg8 | His101 | Tyr6 | Tyr151 | Val7 |
| Asn100 | Tyr6 | Tyr62 | Tyr6 | Asp96 | Thr1 |
| Ala307 | Ile4 | His305 | Arg8 | Gly306 | Pro5 |
| Asn301 | Ile4 | Asp300* | Ile4 | Asp300* | Pro5 |

*Catalytic triad of α-amylase

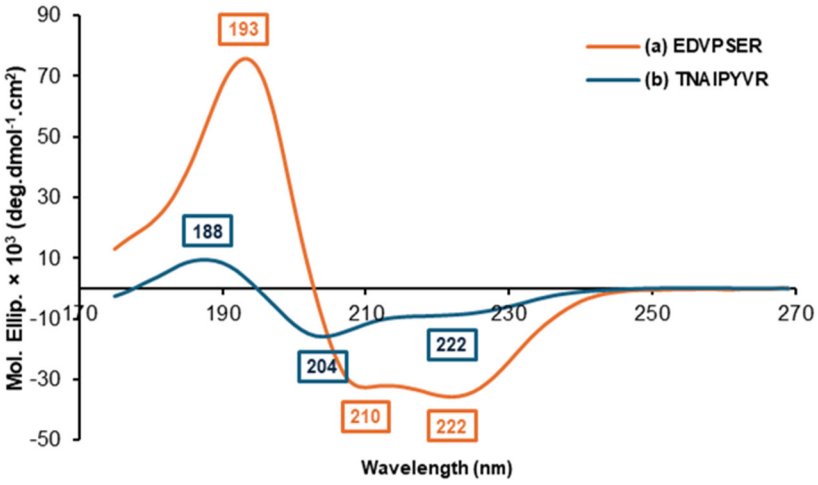


**Fig 4.** Predicted CD spectra of the EDVPSER and TNAIPYVR peptides

the predicted secondary structure based on previous research [40]. EDVPSER exhibited a positive peak at 193 nm and negative peaks at 210 and 222 nm, characteristic of an α-helix, indicating 100% helicity. TNAIPYVR displayed a positive peak at 188 nm, typical of a random coil, along with negative peaks at 204 and 222 nm, suggesting partial α-helix features with an estimated helicity of 20%.

The visualization of the predicted secondary structure of the peptide EDVPSER is presented in Fig. 5. The secondary structure of the peptide was influenced by hydrogen bond interactions formed between the hydrogen atoms of amine groups and the oxygen atoms of carbonyl groups. These hydrogen bonds included an interaction between the carbonyl group of Val3 and the hydrogen atoms of the amine groups of Glu6 and Arg7. Additionally, hydrogen bond interactions were formed between the carbonyl group of Asp2 and the hydrogen atoms of the amine groups of Ser5 and Glu6.

Fig. 6 presents the visualization of the predicted secondary structure of the peptide TNAIPYVR. Hydrogen bond interactions were formed between the carbonyl group of Ile4 and the hydrogen atoms of the amine groups of Val7 and Arg8. These hydrogen bonds contributed to the formation of the α-helix structure. However, the number of hydrogen bonds formed was fewer than those in the peptide EDVPSER. This difference influenced the secondary structure of the peptide, resulting in a secondary structure that was predominantly composed of random coils.

## Synthesis of Peptides

The peptides predicted to have α-amylase inhibitory activity were synthesized using solid-state synthesis to obtain the peptides in solid form. The resulting peptides were white, with a purity of over 90%. The physicochemical properties of the synthesized peptides were predicted using the Peptide Calculator server and confirmed through mass spectrometry and high-performance liquid chromatography (HPLC), as detailed in the attached data.

Table 11 displays the physicochemical properties of the peptides. The peptide EDVPSER exhibited a GRAVY value of −1.886, while TNAIPYVR had a value of −0.138. The GRAVY value reflects hydrophobicity, with higher values indicating greater hydrophobicity [41]. Based on these values, TNAIPYVR was more hydrophobic than EDVPSER. The hydrophobicity of these peptides was

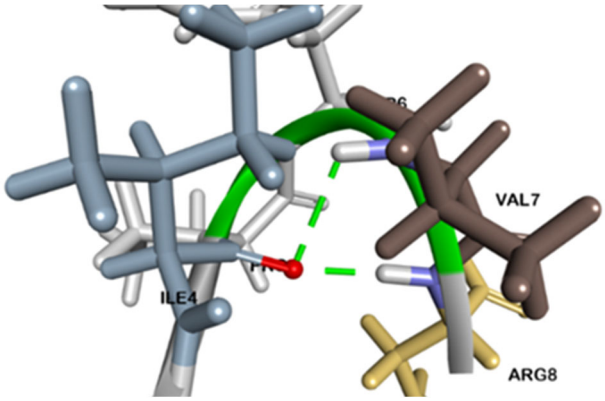


**Fig 6.** Visualization of the predicted secondary structure of the peptide TNAIPYVR

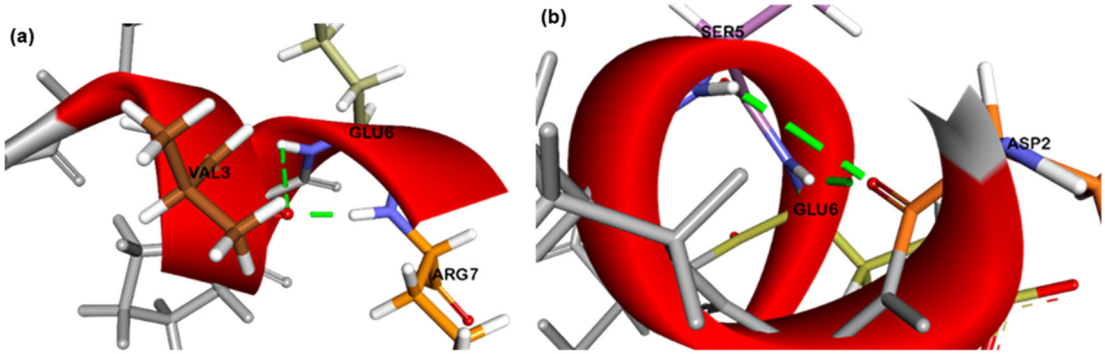


**Fig 5.** Visualization of the predicted secondary structure of the peptide EDVPSER, highlighting hydrogen bond interactions: (a) at Val3, Glu6, and Arg7, and (b) at Asp2, Ser5, and Glu6

**Table 11.** Physicochemical properties of the synthesized peptides predicted through *in silico* analysis

| Amino acids sequence | Number of amino acids | Molecular weight (g/mol) | GRAVY |
|---|---|---|---|
| EDVPSER | 7 | 830.84 | -1.886 |
| TNAIPYVR | 8 | 933.06 | -0.138 |

influenced by their amino acid composition: EDVPSER was dominated by hydrophilic amino acids, while TNAIPYVR contained more hydrophobic amino acids. Hydrophobicity impacted the stability of protein-peptide interactions.

The synthesized peptides EDVPSER and TNAIPYVR showed molecular weights of 830.86 and 933.08 g/mol, closely matching the *in-silico* predictions of 830.84 and 933.06 g/mol, respectively. Chromatograms confirmed purities of 99.18% (EDVPSER) and 95.05% (TNAIPYVR). Both peptides were successfully synthesized with purities above 90%.

### *In Vitro* Antidiabetic Activity Assay of α-Amylase Inhibitors

The hydrolysis of starch by α-amylase reduced starch-iodine complex formation, leading to a decrease in the blue color intensity of the solution. This is evident from the reduced absorbance when comparing a system with only the substrate to one with both enzyme and substrate. The peptide's inhibitory activity can be assessed by the color produced in the solution. The solution will display a bluish-purple color if inhibition occurs, indicating reduced starch hydrolysis. The change in color intensity was measured quantitatively by absorbance at 540 nm using a UV-vis spectrophotometer, where the bluish-purple color was absorbed.

Based on the activity test results (Fig. 7), it was found that both peptides exhibited activity against α-amylase. This was demonstrated by the appearance of a purple color in the system solution when the iodine solution was added. The color change indicates the formation of a starch-iodine complex, suggesting that the starch in the system was not hydrolyzed into simpler glucose molecules.

The peptides obtained from *in silico* digestion were compared to a known α-amylase inhibitor bioactive peptide derived from plants, YFDEQNEQFR, has an $IC_{50}$ value of 37.5 ± 1.1 μM [9]. According to Table 12, the peptide EDVPSER exhibited a lower $IC_{50}$ value than YFDEQNEQFR, suggesting that the *in silico* digestion-derived peptide could inhibit enzyme activity more effectively than YFDEQNEQFR.

Starch was hydrolyzed into simpler glucose molecules through two stages. The first stage involved the interaction between the protein and starch to direct the glucose chain (oligosaccharide) toward the active site of α-amylase. Amino acids such as Trp59, Tyr62, and Tyr151 were involved in this stage. The second stage was hydrolysis, involving Asp197, Glu233, and Asp300. In addition to the catalytic triad, other amino acids like Trp59, Tyr62 [21], and Tyr151 [9] also played roles in starch hydrolysis. Inhibiting these amino acids could enhance the peptide's inhibitory effect on α-amylase.

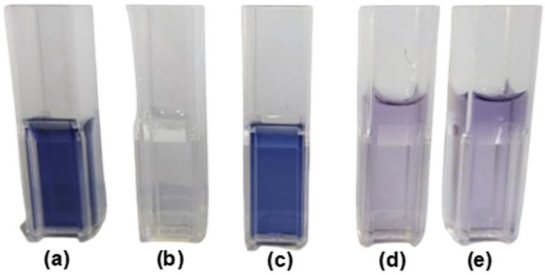


**Fig 7.** The color changes in the solution system were as follows: (a) blank, (b) control, (c) $S_0$, (d) $S_1$ TNAIPYVR, and (e) $S_1$ EDVPSER

**Table 12.** $IC_{50}$ values of acarbose and peptides

| Sample | $IC_{50}$ (μM) | | | Average | SD |
|---|---|---|---|---|---|
| | 1 | 2 | 3 | | |
| Acarbose | 57.11 | 58.70 | 57.20 | 57.67 | 0.73 |
| EDVPSER | 13.24 | 14.62 | 14.62 | 14.16 | 0.65 |
| TNAIPYVR | 78.17 | 78.01 | 73.58 | 76.58 | 2.13 |

The inhibitory potential of the *in-silico* digestion-derived peptides against α-amylase was related to the enzyme inhibition mechanism. This mechanism is based on the peptide's ability to form barriers through hydrogen bonding interactions with residues around the substrate-binding region [6]. Hydrogen interactions are critical in protein-peptide interactions, as they are common in the formation of protein-peptide complexes and have a stronger effect compared to other intermolecular interactions.

Molecular docking studies of the peptide EDVPSER with α-amylase revealed hydrogen bond interactions with non-catalytic triad amino acids, such as Tyr151, which played an important role in the starch hydrolysis mechanism. Interactions at Trp59 were identified as π-alkyl interactions, and Van der Waals interactions were observed at Tyr62. Meanwhile, the peptide "TNAIPYVR" did not exhibit hydrogen bond interactions at Trp59, Tyr62, or Tyr151. The interactions formed at Trp59 were Van der Waals interactions, at Tyr62, π-cation interactions were found, and at Tyr151, π-alkyl and T-shaped π-π interactions were observed.

Previous studies on bioactive peptides indicate that certain amino acids in bioactive peptides play a crucial role in inhibiting the catalytic triad of α-amylase. Proline, leucine, and serine are three reactive amino acids in bioactive peptides [23]. In addition to hydrogen bonding interactions, Cα-H···π interactions (aromatic π, amide, or arginine) were also frequently found to explain the formation of protein-ligand complexes. However, this interaction was not observed in the molecular docking results, even though proline and serine were present in EDVPSER, and proline was present in TNAIPYVR.

Although proline, leucine, and serine did not form Cα-H···π interactions, they still contribute to protein-peptide stability [23]. Proline is hydrophobic, nonpolar, and aliphatic, while serine is hydrophilic, polar, and aliphatic. Hydrophobic amino acids interact stably with enzymes due to hydrophobic pockets, reducing susceptibility to degradation. Serine's role is supported by its polar nature, which influences hydrogen bond formation. Additionally, the aliphatic nature of serine and proline contributes to stability by reducing steric hindrance and enhancing flexibility.

The peptides EDVPSER and TNAIPYVR demonstrated effective interactions with α-amylase, as confirmed by *in vitro* assays. Peptide EDVPSER exhibited superior inhibitory activity, likely due to the active roles of proline and serine and its hydrogen bond interactions with key residues such as Tyr151. These findings highlight EDVPSER as a promising candidate for further research and development of antidiabetic treatments derived from goat milk proteins.

## ■ CONCLUSION

*In silico* protein cleavage efficiently identified bioactive peptides. In this study, peptides from goat milk casein were analyzed for α-amylase inhibition. The peptide EDVPSER ($\alpha_{s1}$-casein) showed strong inhibitory potential, supported by molecular docking revealing interactions with the catalytic triad. EDVPSER had a superior $IC_{50}$ value compared to acarbose and YFDEQNEQFR. In contrast, TNAIPYVR ($\alpha_{s2}$-casein) exhibited lower activity. Hydrogen bonding at the catalytic triad was crucial for inhibition. This study highlighted *in silico* methods as effective tools for identifying and predicting bioactive peptides.

## ■ ACKNOWLEDGMENTS

The author would like to extend their deepest gratitude to the Ministry of Education, Culture, Research, and Technology of the Republic of Indonesia (Kementerian Pendidikan, Kebudayaan, Riset, dan Teknologi Republik Indonesia) and Directorate of Research of Universitas Gadjah Mada under agreement number 048/E5/PG.02.00.PL/2024 and 2662/UN1/DITLIT/PT.01.03/2024 for providing the financial support that made this research possible. This generous funding has been instrumental in the completion of this study. The authors deeply appreciate the continued commitment to advancing scientific research.

## ■ CONFLICT OF INTEREST

The authors declare that there is no conflict of interest regarding the publication of this paper.

## ■ AUTHOR CONTRIBUTIONS

Gavriel Hagai Paulus Sumlang conducted the *in-silico* digestion analysis, molecular docking, activity assay, and the preparation of the manuscript. Tri Joko Raharjo was responsible for the conceptualization, review, and supervision. Marlyn Dian Laksitorini and Endang Astuti contributed to the review and supervision. Rumaisha Lale Handoyo conducted the molecular docking and activity assay. All authors agreed to the final version of this manuscript.

## ■ REFERENCES

[1] Berraquero-Garcia, C., Rivero-Pino, F., Ospina, J.L., Pèrez-Galvez, R., Espejo-Carpio, F.J., Guadix, A., Garcia-Moreno, P.J., and Guadix, E.M., 2023, Activity, structural features and *in silico* digestion of antidiabetic peptides, *Food Biosci.*, 55 (19), 102954.

[2] Khan, M.A.B., Hashim, M.J., King, J.K., Govender, R.D., Mustafa, H., and Kaabi, J.A., 2020, Epidemiology of type 2 diabetes – Global burden of disease and forecasted trends, *J. Epidemiol. Global Health*, 1 (10), 107–111.

[3] Chandrasekaran, P., and Weiskirchen, R., 2024, The role of obesity in type 2 diabetes mellitus – An overview, *Int. J. Mol. Sci.*, 25 (3), 1882.

[4] Famuwagun, A.A., Alashi, A.M., Gbadamosi, O.S., Taiwo, K.A., Oyedele, D., Adebooye, O.C., and Aluko, R.E., 2021, Antioxidant and enzymes inhibitory properties of Amaranth leaf protein hydrolyzates and ultrafiltration peptide fractions, *J. Food Biochem.*, 45 (3), e13396.

[5] Dujic, T., Causevic, A., Bego, T., Malenica, M., Velija-Asimi, Z., Pearson, E.R., and Semiz, S., 2015, Organic cation transporter 1 variants and gastrointestinal side effects of metformin in patients with type 2 diabetes, *Diabetic Med.*, 33 (4), 511–514.

[6] Fadimu, G.J., Gill, H., Farahnaky, A., and Truong, T., 2022, Improving the enzymolysis efficiency of lupin protein by ultrasound pretreatment: Effect on antihypertensive, antidiabetic and antioxidant activities of the hydrolysates, *Food Chem.*, 383, 132457.

[7] Singh, B.P., Paul, S., and Goel, 2024, Shotgun proteomics and molecular simulations on multifunctional bioactive peptides derived from the whey of unexplored "Gaddi" goat of Himalayas, *Food Chem.*, 430, 137075.

[8] Martini, S., Solieri, L., Cattivelli, A., Pizzamiglio, V., and Tagliazucchi, D., 2021, An integrated peptidomics and *in silico* approach to identify novel anti-diabetic peptides in Parmigiano-Reggiano cheese, *Biology*, 10 (6), 563.

[9] Esfandi, R., Seidu, I., Willmore, W., and Tsopmo, A., 2022, Antioxidant, pancreatic lipase, and α-amylase inhibitory properties of oat bran hydrolyzed proteins and peptides, *J. Food Biochem.*, 46 (4), e13762.

[10] Guetouache, M., Guessas, B., and Medjekal, S., 2014, Composition and nutritional value of raw milk, *Biol. Sci. Pharm. Res.*, 10 (2), 115–122.

[11] Al Mazroea, A., Alharby, M.A., Almughatwai, A.A., Al-Remaithi, S.M., Saeed, R.M., Alharbi, A.F., and Saeed, H.M., 2018, Comparison between nutritional values in cow's milk, and goat milk infant formulas, *Int. J. Pharm. Res. Allied Sci.*, 4 (7), 190–195.

[12] Wang, Z., Jiang, S., Ma, C., Huo, D., Peng, Q., Shao, Y., and Zhang, J., 2018, Evaluation of the nutrition and function of cow and goat milk based on intestinal microbiota by metagenomic analysis, *Food Funct.*, 4 (9), 2320–2327.

[13] Campos, M.I.F., Barbosa, P.P., Camargo, L.J., Pinto, L.D., Mataribu, B., Serrão, C., Marques-Santos, L.F., Lopes, J.H., Oliveira, J.M.G., Gadelha, C.A., and Santi-Gadelha, T., 2022, Characterization of goat whey proteins and their bioactivity and toxicity assay, *Food Biosci.*, 46, 101591.

[14] Barati, M., Javanmardi, F., Jabbari, M., Mokari-Yamchi, A., Farahmand, F., Eş, I., Farhadnejad, H., Davoodi, S.H., and Khaneghah, A.M., 2020, An *in silico* model to predict and estimate digestion-resistant and bioactive peptide content of dairy products: A primarily study of a time-saving and affordable method for practical research purposes, *LWT*, 130, 109616.

[15] Kęska, P., Stadnik, J., Łupawka, A., and Michalska, A., 2023, Novel α-glucosidase inhibitory peptides identified *in silico* from dry-cured pork loins with

probiotics through peptidomic and molecular docking analysis, *Nutrients*, 15 (16), 3539.

[16] Weng, G., Gao, J., Wang, Z., Wang, E., Hu, X., Yao, X., Cao, D., and Hou, T., 2020, Comprehensive evaluation of fourteen docking programs on protein–peptide complexes, *J. Chem. Theory Comput.*, 16 (6), 3959–3969.

[17] Ciemny, M., Kurcinski, M., Kamel, K., Kolinski, A., Alam, N., Schueler-Furman, O., and Kmiecik, S., 2018, Protein–peptide docking: Opportunities and challenges, *Drug Discovery Today*, 23 (8), 1530–1537.

[18] Choi, S., Son, S.H., Kim, M.Y., Na, I., Uversky, V.N., and Kim, C.G., 2023, Improved prediction of protein-protein interactions by a modified strategy using three conventional docking software in combination, *Int. J. Biol. Macromol.*, 252, 126526.

[19] Trabuco, L.G., Lise, S., Petsalaki, E., and Russel, R.B., 2012, PepSite: Prediction of peptide-binding sites from protein surfaces, *Nucleic Acids Res.*, 40 (W1), W423–W427.

[20] Fadimu, G.J., Farahnaky, A., Gill, H., Olalere, O.A., Gan, C.Y., and Truong, T., 2022, *In silico* analysis and antidiabetic effect of α-amylase and α-glucosidase inhibitory peptides from lupin protein hydrolysate: Enzyme-peptide interaction study using molecular docking approach, *Foods*, 11 (21), 3375.

[21] Evaristus, N.A., Wan Abdullah, W.N., and Gan, C.Y., 2018, Extraction and identification of α-amylase inhibitor peptides from *Nephelium lappacheum* and *Nephelium mutabile* seed protein using gastro-digestive enzymes, *Peptides*, 102, 61–67.

[22] Huang, Y., Richardson, S.J., Brennan, C.S., and Kasapis, S., 2024, Mechanistic insights into α-amylase inhibition, binding affinity and structural changes upon interaction with gallic acid, *Food Hydrocolloids*, 148, 109467.

[23] Mohd Rodhi, A., Yap, P.G., Olalere, O.A., and Gan, C.Y., 2024, Unveiling α-amylase inhibition: A bioinformatics perspective on peptide properties and amino acid contributions, *J. Mol. Struct.*, 1305, 137768.

[24] Honorato, R.V., Trellet, M.E., Jiménez-García, B., Schaarschmidt, J.J., Giulini, M., Reys, V., Koukos, P.I., Rodrigues, J.P.G.L.M., Karaca, E., van Zundert, G.C.P., Roel-Touris, J., van Noort, C.W., Jandová, Z., Melquiond, A.S.J., and Bonvin, A.M.J.J., 2024, The HADDOCK2.4 web server for integrative modeling of biomolecular complexes, *Nat. Protoc.*, 19 (11), 3219–3241.

[25] Honorato, R.V., Koukos, P.I., Jiménez-García, B., Tsaregorodtsev, A., Verlato, M., Giachetti, A., Rosato, A., and Bonvin, A.M.J.J., 2021, Structural biology in the clouds: The WeNMR-EOSC ecosystem, *Front. Mol. Biosci.*, 8, 729513.

[26] Kurcinski, M., Jamroz, M., Blaszczyk, M., Kolinski, A., and Kmiecik, S., 2015, CABS-dock web server for the flexible docking of peptides to proteins without prior knowledge of the binding site, *Nucleic Acid Res.*, 43 (W1), W419–W424.

[27] Benoit, S., Chaumontet, C., Violle, N., Boulier, A., Hafeez, Z., Cakir-Kiefer, C., Tomé, D., Schwarz, J., and Miclo, L., 2022, The anxiolytic-like properties of a tryptic hydrolysate of bovine $\alpha_{s1}$ casein containing α-casozepine rely on $GABA_A$ receptor benzodiazepine binding sites but not the vagus nerve, *Nutrients*, 14 (11), 2212.

[28] Shanmugam, V.P., Kapila, S., Sonfack, T.K., and Kapila, R, 2015, Antioxidative peptide derived from enzymatic digestion of buffalo casein, *Int. Dairy J.*, 42, 1–5.

[29] Zhang, Y., Wang, N., Wang, W., Wang, J., Zhu, Z., and Li, X., 2016, Molecular mechanisms of novel peptides from silkworm pupae that inhibit α-glucosidase, *Peptides*, 76, 45–50.

[30] Reddi, S., Shanmugam, V.P., Tanedjeu, K.S., Kapila, S., and Kapila, R., 2018, Effect of buffalo casein-derived novel bioactive peptides on osteoblast differentiation, *Eur. J. Nutr.*, 57 (2), 593–605.

[31] McClean, S., Beggs, L.B., and Welch, R.W., 2014, Antimicrobial activity of antihypertensive food-derived peptides and selected alanine analogues, *Food Chem.*, 146, 443–447.

[32] Sedaghati, M., Ezzatpanah, H., Mashhadi Akbar Boojar, M., Tajabadi Ebrahimi, M., and Kobarfard, F., 2016, Isolation and identification of some antibacterial peptides in the plasmin-digest of β-casein, *LWT - Food Sci. Technol.*, 68, 217–225.

[33] Kumar, N., Devi, S., Mada, S.B., Reddi, S., Kapila, R., and Kapila, S., 2020, Anti-apoptotic effect of buffalo milk casein derived bioactive peptide by directing Nrf2 regulation in starving fibroblasts, *Food Biosci.*, 35, 100566.

[34] Kumar, N., Reddi, S., Devi, S., Mada, S.B., Kapila, R., and Kapila, S., 2019, Nrf2 dependent antiaging effect of milk-derived bioactive peptide in old fibroblasts, *J Cell Biochem.*, 120 (6), 9677–9691.

[35] Plaisancié, P., Boutrou, R., Estienne, R., Henry, G., Jardin, J., Paquet, A., and Léonil, J., 2015, β-Casein(94-123)-derived peptides differently modulate production of mucins in intestinal goblet cells, *J. Dairy Res.*, 82 (1), 36–46.

[36] Chiba, H., Tani, F., and Yoshikawa, M., 1989, Opioid antagonist peptides derived from κ-casein, *J. Dairy Res.*, 56 (3), 363–366.

[37] Helmy, M.W., Youssef, M.H., Yamari, I., Amr, A., Moussa, F.I., El Wakil, A., Chtita, S., El-Samad, L.M., and Hassan, M.A., 2024, Repurposing of sericin combined with dactolisib or vitamin D to combat non-small lung cancer cells through computational and biological investigations, *Sci. Rep.*, 14 (1), 27034.

[38] Chen, D., Oezguen, N., Urvil, P., Ferguson, C., Dann, S.M., and Savidge, T.C., 2016, Regulation of protein-ligand binding affinity by hydrogen bond pairing, *Sci. Adv.*, 2 (3), e1501240.

[39] Nagy, G., and Grubmuller, H., 2021, Implementation of a Bayesian secondary structure estimation method for the SESCA circular dichroism analysis package, *Comput. Phys. Commun.*, 266, 108022.

[40] Marella, S., 2018, Antidiabetic plant proteins/peptides as complementary and alternative medicine – Analytical perspectives, *Rev. Anal. Chem.*, 37 (4), 20170025.

[41] Fillería, S.G., Nardo, A.E., Paulino, M., and Tironi, V., 2021, Peptides derived from the gastrointestinal digestion of amaranth 11S globulin: Structure and antioxidant functionality, *Food Chem.: Mol. Sci.*, 3, 100053.